Physics of Transition Metal Oxides

Lecture 11

Defects in oxides

Defects in oxides:

We have looked at a variety of defects already. Today we discuss

- structural defects, giving rise to distinct phases
- impurity defects, which modify the properties of the parent crystal

The most common defect types:

- lattice vacancies

- interstitial atoms

Combinations are also possible

- Frenkel (vacancy plus an interstitial of the same ion)

- Schottky (vacancies of both types)

A special feture of oxides is that the lattice can accommodate a very high concentration of defects.

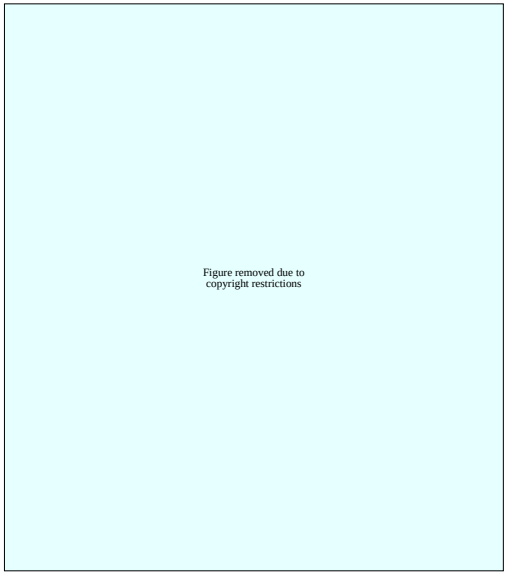

Cox92 p.13

Determining defect type is not easy. Diffraction techniques and direct TEM observation can be used when concentrations are high. Studying isolated defects or materials with very low defect densities is much harder.

Simple point defects appear to be rather unusual, because they have a nonzero charge and thus long-range Coulomb interactions. The point defect model works in some cases, such as wüstite, $Fe_{1-x}O$. The basic structure is rock-salt:

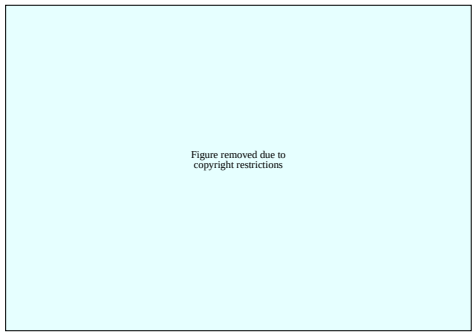

Cox92 p.27

Long-range interactions are responsible for defect clustering. Fe atoms appear to be in tetrahedral sites in addition to the expected octahedral sites. This is well-known for Fe_3O_4, of course. The clusters that have been proposed are shown in this figure. $\circ$ is the Fe^{2+} vacancy site, $\triangle$ is the interstitial Fe^{3+} site.

Larger deviation from stoichiometry results in the presence of larger clusters.

At high defect concentrations we may also see cluster ordering.

A large concentration of Schottky defects results in a reduced density of the whole crystal (lower than the density calculated from the x-ray diffraction unit cell dimensions).

Creating a defect requires a large amount of energy (≈2 eV). Intrinsic defect concentration is thus very low, $\sim 10^{-5}$ at 0.8 T_m.

Vacancy formation reaction in a binary oxide $M_{1-x}O$ (M is a divalent ion) has an equilibrium constant

$$K_{V_M^{2+}} = 4x^3 P_{O_2}^{-1/2}$$

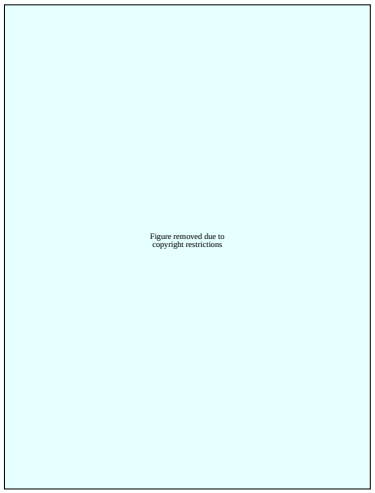

Rao98 p.16

The composition of the oxide depends on the oxygen partial pressure as given by $x \propto P_{O_2}^{1/6}$ (For doubly ionized vacancies). If the vacancies are singly ionized, then $x \propto P_{O_2}^{1/4}$.

We look at the partial molar free energy of oxygen,

$$\Delta G_{O_2} = RT \ln P_{O_2}$$

and we can thus write

$$\Delta G_{O_2} = nRT \ln x.$$

The ΔG data comes from thermogravimetric analysis and a plot of ΔG vs. $\ln x$ should be linear with a slope of $n = 6$ for V_M^{2-} or $n = 4$ for V_M^{-}.

- $n = 6$ (doubly ionized vacancies) This slope appears at $x \geq 0.09$.
- $n = 5$ ($[V_M - V_M]^{4-}$ pairs) is seen in a similar concentration range
- $n = 3$ and $n = 4$ appear at $x < 0.09$. These have been assigned to $[4V_M^{2-} - Fe_i^{3+}]^{5-}$ and $[16V_M^{2-} - 5Fe_i^{3+}]^{17-}$ defect complexes. The 16:5 complex is similar to the Fe_3O_4 structure.

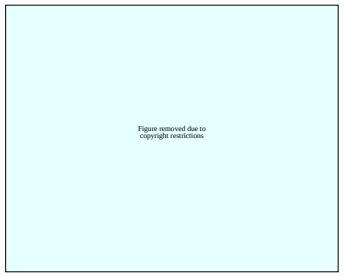

Similar vacancy structures exist in TiO, VO, and MnO systems. The type of vacancy + interstitial shown here is more common in VO, where each interstitial is surrounded by four cation vacancies.

Rao98 p.17

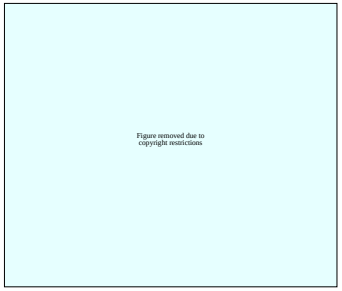

A larger cluster of Fe vacancies and interstitials is shown here. Identification is based on x-ray diffraction of quenched $Fe_{0.9}O$ crystals. The cluster has four tetrahedral Fe^{3+} sites and 13 vacancies at the Fe^{2+} sites. The cluster has a net charge, but the oxide lattice is not disturbed and it can therefore exist in an otherwise ideal rock-salt lattice.

Rao98 p.17

As x changes in $Fe_{1-x}O$, we would thus get a sequence

isolated vacancies → dipolar associates → 4:1 clusters → 6:2, 8:3, 13:4, and larger clusters → corner-shared 16:5 clusters → Fe_3O_4 inverse spinel structure.

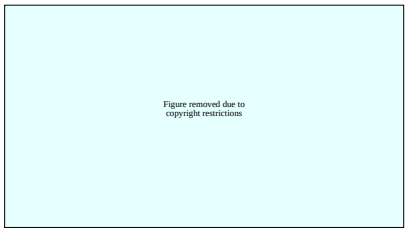

Similar vacancy structures also exist in TiO_x with $0.7 \leq x \leq 1.25$. Several microphases exist. Instead of interstitial oxygens, the structure has a titanium-deficient structure. The lattice of $TiO_{1.25}$ is tetragonal. The figure shows Ti:•, oxygen:◯, vacancies:⊗. The two plots are for height $z = 0$ and $z = 1/2$.

Rao98 p.32

Two of 12 titanium sites are vacant in an ordered way. The structural formula is $(Ti_{10}\square_2)O_{12}$.

Even stoichiometric TiO has a high density of defects, with 15% of Ti and O sites vacant, i.e. the density of the crystal is lower than expected. Ordering of vacancies usually occurs below 900 K.

So far we looked at vacancies and interstitials of metal ions. It is also possible to have extra oxygen, as in $LaMnO_{2+\delta}$. The material usually contains about 12% of Mn^{4+}, attributed to anion excess (extra oxygen). It is not clear where the extra oxygen is, and apparently at least some of the Mn^{4+} is due to vacancies in A and B sites (La and Mn)

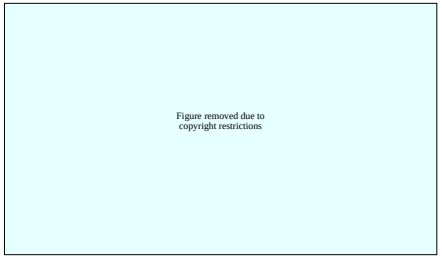

It is also possible to have oxygen deficiency in the lattice. An example is $SrFeO_3$. At high temperature 1/6 of all oxygen sites are randomly empty. Vacancy ordering occurs below 1100 K. The ordered lattice has a *brownmillerite structure*, which is an intergrowth of $(ABO_3)_n \cdot ABO_2$ type.

Rao98 p.47

The tetrahedral layers are missing rows of oxygen along the $< 110 >$ direction. An empty oxygen row alternates with a filled oxygen row.

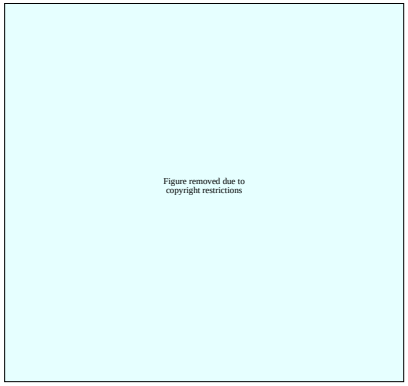

Various d^0 Ti, V, Nb, Mo, and W oxides avoid the formation of point defects due to the presence of shear planes. This eliminates a whole plane of oxgen defects from the crystal, as shown here for the basic ReO_3 structure. The shear plane also turns some corner-sharing octahedra into edge-sharing octahedra.

Cox92 p.28

Such defect planes are not neutral, but this problem is balanced by polarization of the lattice around the defects. Most of these oxides have a large dielectric constant, which results from a large lattice polarizability. It is also possible that direct metal-metal bonding is important.

Shear planes exist in TiO_2 for example, even for very small oxygen loss, as in $TiO_{1.997}$.

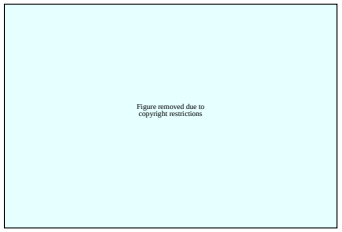

Shear planes are responsible for a wide variety of oxide compositions. This example shows the structure of Mo_8O_{23}. The general formula is Mo_nO_{3n-1}.

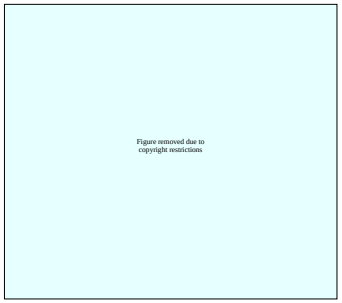

The shear structures can be ordered and result in very large unit cells, such as the $W_{20}O_{58}$ lattice shown here. This is the smallest member in the W_nO_{3n-2} family. Other known phases have $n = 20, 24, 25, 40$.

Rao98 p.197,198

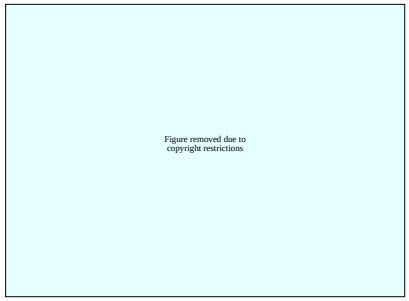

Rao98 p.20

The shear planes discussed here are just one form of *dislocations* that can occur in oxides. Ordered vacancies or shear planes result in distinct phases. There are various other dislocations that are usually not ordered and do not result in distinct crystal phases, but they can still have a dramatic effect on the crystal properties.
The most common dislocation type is an edge dislocation, i.e. the insertion of an extra row of atoms. The example here is a TEM image of $Ba_2Bi_4Ti_5O_{18}$.

Other very common dislocations are screw dislocations, and grain boundaries. Oxides occasionally also have *stacking faults* where a single atomic layer is missing from a crystal. Arrays of dislocations give rise to *tilt boundaries* (array of periodically spaced edge dislocations) or *twist boundaries* (arrays of screw dislocations). Noncubic crystals often show *twinning*.

Impurities in oxides

We now look at how impurity atoms in an oxide lattice affect its properties. Mostly we look at the effects of d^n ions in oxides like MgO, Al_2O_3 or TiO_2. Such impurity ions are almost always present, even in 'pure' crystals. the most common effect is to give a slight shade of color to otherwise transparent crystals. The dilute impurity systems are useful for studying the energy levels of d^n ions. Similar level diagrams apply also to more concentrated systems (where we would talk about intentional %-level doping).

The most useful techniques for studying impurity states are

- **optical spectroscopy** Measures the energies of crystal field and charge transfer transitions
- **ESR** Measures the ground state magnetic properties

Here we see the absorption spectrum of Cr^{3+} impurities in Al_2O_3.

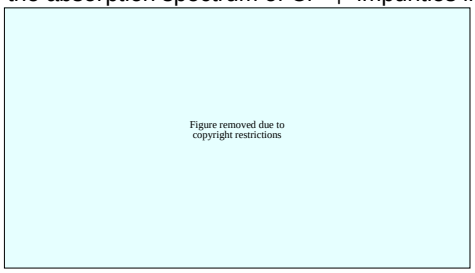

Cox92 p.45

The Cr^{3+} ion has 3 d-electrons and the ground state spectroscopic term is $^4A_{2g}$. Selection rules define the shape of the spectrum. The allowed transitions give strong absorption around 2-3 eV. Transitions to the ^2E levels are much weaker and only visible because the ground state is actually a slightly distorted octahedron.

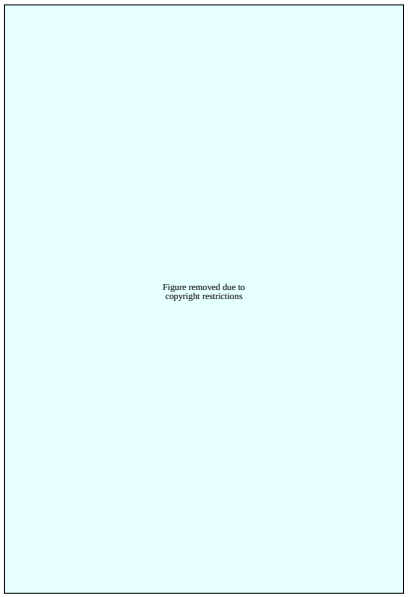

Cox92 p.119

When ruby is illuminated in the ^2E band, we get a weak emission spectrum. These are the R-lines that were the basis for the first laser.
The energy of an electronic state depends on the Cr-O distance as shown in the energy levl diagram. Distances change due to local vibration modes. the $^4T_2$ levels correspond to an electronic excitation to the t^2e^1 configuration, i.e. an electron has been excited from the t levels to an antibonding e level. The equilibrium bond length for that levels is thus larger. The ^2E and $^2T_2$ correspond to rearrangement of electrons within the t levels and therefore there is no bond length change associated with the transition.
According to the *Frank-Condon* principle, electronic transitions are faster than ionic rearrangements. The transition to $^4T_2$ is thus accompanied by a vibronic excitation, which broadens the line. The ^2E and ^2T transitions do not suffer from vibronic excitations and they are therefore much sharper.

Absorption of Cr^{3+} is rather different in a TiO_2 crystal, where the absorption band shifts towards the red part of the spectrum (from 14000 to 18000 cm^{-1}). This shows that the crystal-field splitting is smaller.

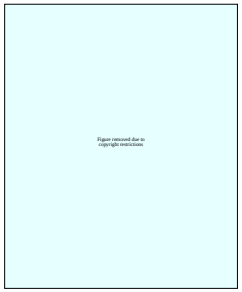

Understanding the structure of optical spectra usually requires some knowledge of the ground state. This information can be obtained from *electron spin resonance*, ESR. (or EPR, electron paramagnetic resonance).

Blundell01 p.60

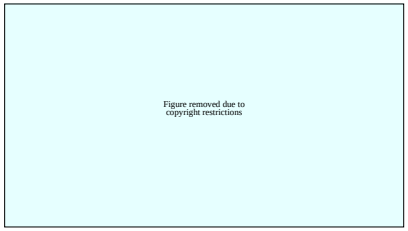

This would be an example of a $J = 1$ ion like Ni^{2+}. If there is no crystal field splitting, we would get a single absorption line. Usually there is at least some splitting, and we get a multiplet of lines. By counting the number of absorption lines we get an idea of what the ground state spin configuration is.

ESR has been used to determine the spin states of various impurity ions in common oxides.

MgO				$SrTiO_3$			
Ti^+							
	V^{2+}	V^{3+}				V^{4+}	
	Cr^{2+}	Cr^{3+}			Cr^{3+}		Cr^{5+}
	Mn^{2+}		Mn^{4+}	Mn^{2+}		Mn^{4+}	
Fe^+	Fe^{2+}	Fe^{3+}		Fe^{2+}	Fe^{3+}	Fe^{4+}	Fe^{5+}
Co^+	Co^{2+}				Co^{3+}		
Ni^+	Ni^{2+}	Ni^{3+}		Ni^{2+}	Ni^{3+}	Ni^{4+}	

Cox92 p.121

Some ions can not be measured by ESR, such as low-spin Co^{3+}, which has a closed-shell t_{2g}^6 configuration with $S = 0$. In other cases, like Mn^{3+}, relaxation effects appear to be so fast that lines are very broad and components cannot be resolved.

ESR measurements show that in most cases impurities occupy substitutional sites, such as Mg^{2+} in MgO and Ti^{4+} in TiO_2. If a nonmatching substitution takes place, such as Cr^{3+} at a Mg^{2+} site, then we need additional defects to compensate for the charge imbalance. This can lead to defect clustering, where a substitutional Cr^{3+} and a Mg^{2+} vacancy are at neighboring sites. Isolated Cr^{3+} defects are only found at concentrations below 0.02%. Above that, (Cr^{3+})-(Mg^{2+} vacancy) pairs start to form. Substitutional metals may also be paired with an oxygen vacancy (as happens in $SrTiO_3$).

Charge transfer energies

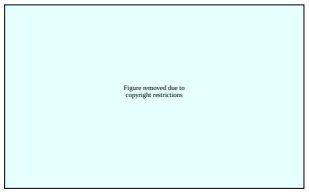

Cox92 p.52

The enrgy levels of an isolated d^n ion can be determined quite nicely, as we have seen. A more difficult problem is to measure the energies with respect to the bands of the host crystal.
This is necessary to understand transitions where an electron is excited from the impurity to the conduction band, or from the valence band into an impurity state.

These transitions can be much stronger than the $d - d$ transitions that we looked at earlier. Charge transfer transitions can also create free carriers, giving semiconductions (thermal excitation) or photoconductivity (optical excitation). The added carriers can alter other properties of the crystal, like the photorefractive effect in $LiNbO_3$.

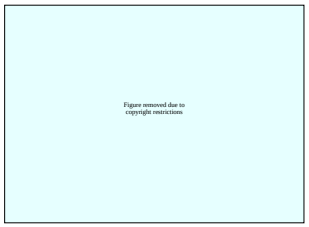

This plot shows the absorption spectrum of Ni^{2+} ions in MgO. The crystal-field transitions are at 3 eV and rather weak. The charge-transfer transitions at 6 eV is much stronger, just below the band gap of 7.5 eV.

Cox92 p.121

The transfer reaction could be either

$$Ni^{2+} = Ni^{+} + h^{+}$$

or

$$Ni^{2+} = Ni^{3+} + e^{-}$$

The former reaction is more probable. Problems are caused by other transitions from other types of defects, which must be in the crystal to compensate for the charge imbalance caused by the impurity.

In priciple, it should be possible to calculate the energy levels of the impurity relative to the band edges of the host lattice. The difficulty lies in knowing the precise lattice distortions that occur close to an impurity atom. These are not known.

How to show the impurity levels in a host material band diagram

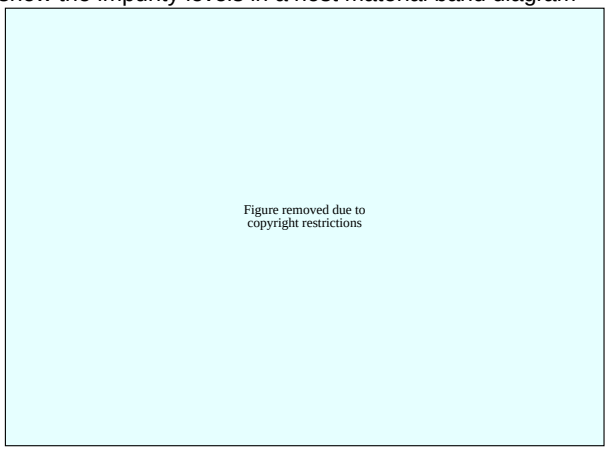

Cox92 p.125

(a) shows the crystal field splitting for an appropriate octahedral site. This is acceptable only for a d^0 ion, since it doesn't show the electrons in the levels.

(b) specifies also the orbital occupancy. This still doesn't show the spectroscopic states. Electronic repulsion changes in excited states.

(c) adds spin-dependent exchange splitting (between up and down spin states).

(d) is a rather simple 'chemical' view, ignoring individual orbitals and only showing energies of different oxidation states. The Fe^{2+}/Fe^{3+} level position gives the energies for these reactions:

$$Fe^{2+} = Fe^{3+} + e^-$$

or

$$Fe^{3+} = Fe^{2+} + h^+$$

This assumes that we look at the ground states only. This picture is useful for estimating donor or acceptor ionization energies in semiconducting materials but doesn't help for the analysis of optical spectra.

(e) is a simplified view of case (d). The labels usually treat all impurities as donors, i.e. Fe^{3+} stands for a Fe^{4+}/Fe^{3+} transition, not the Fe^{3+}/Fe^{2+} transition.

(f) shows the ground states and the excited crystal field levels above the ground states. This is useful in semiconductors to understand all the possible transition energies.

(g) shows the effects of vibrational excitations. These are very important in oxides, because the geometries of the charge transfer ground and excited states can be quite different. The width of the Gaussian would give an estimate of the distribution expected from the Franck-Condon principle.

There are four possible reactions

$$Fe^{2+} = Fe^{3+} + e^- \quad (1)$$
$$Fe^{2+} + h^+ = Fe^{3+} \quad (2)$$
$$Fe^{3+} = Fe^{2+} + h^+ \quad (3)$$
$$Fe^{3+} + e^- = Fe^{2+} \quad (4)$$

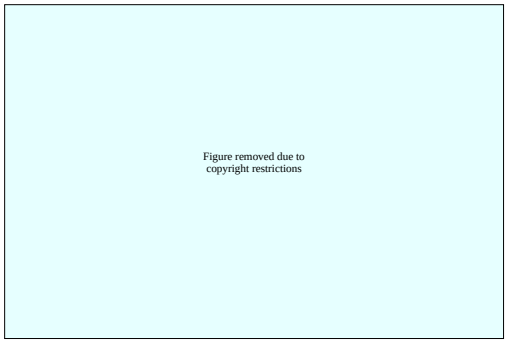

Cox92 p.128

This figure shows systematic behavior of impurities in TiO_2. For a fixed d electron configuartion, we see a stabilization of about 2 eV as the nuclear charge increases from one element to the next. Changes of d electron numbers couse more erratic energy differences due to the competition of crystal field and exchange terms.

The energy changes between different valence states of the same element is the result of electron repulsion (which gets stronger as electrons are added). This energy difference gives an estimate for the Hubbard U. The plot shows that U is around 1 to 3 eV.

Interactions between impurities:

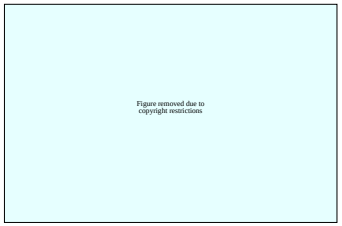

Cox92 p.130

Interactions between Cr^{3+} impurities in ruby have been measured. It appears that impurities form pairs, which order antiferromagnetically. The ground state of each Cr atom has a spin of $S = 3/2$. The combined defect pair thus has spin values 0, 1, 2, 3, 4, with $S = 0$ having the lowest energy. The splitting energies are very small, only about 100 cm^{-1}, or 10 meV. This is understandable, and shows that direct coupling between two metals at neighboring lattice sites is very weak. The coupling energy is much smaller than CF or CT energies.